Impact of SBRT fractionation in hypoxia dose painting - Accounting for heterogeneous and dynamic tumor oxygenation

Impact of SBRT fractionation in hypoxia dose painting — Accounting for heterogeneous and dynamic tumor oxygenation

Emely Kjellsson Lindblom[a)] and Ana Ureba
Medical Radiation Physics, Department of Physics, Stockholm University, Stockholm S-17176, Sweden

Alexandru Dasu
The Skandion Clinic, Uppsala S-75237, Sweden

Peter Wersäll
Department of Oncology, Karolinska University Hospital, Stockholm S-17176, Sweden

Aniek J. G. Even, Wouter van Elmpt, and Philippe Lambin
Department of Radiation Oncology (MAASTRO), GROW-School for Oncology and Developmental Biology, Maastricht University Medical Center, Maastricht 6229, The Netherlands

Iuliana Toma-Dasu
Medical Radiation Physics, Department of Physics, Stockholm University, Stockholm S-17176, Sweden
Medical Radiation Physics, Department of Oncology and Pathology, Karolinska Institutet, Stockholm S-17176, Sweden

(Received 5 July 2018; revised 18 February 2019; accepted for publication 13 March 2019; published 14 April 2019)

Purpose: Tumor hypoxia, often found in nonsmall cell lung cancer (NSCLC), implies an increased resistance to radiotherapy. Pretreatment assessment of tumor oxygenation is, therefore, warranted in these patients, as functional imaging of hypoxia could be used as a basis for dose painting. This study aimed at investigating the feasibility of using a method for calculating the dose required in hypoxic subvolumes segmented on ^{18}F-HX4 positron emission tomography (PET) imaging of NSCLC.
Methods: Positron emission tomography imaging data based on the hypoxia tracer ^{18}F-HX4 of 19 NSCLC patients were included in the study. Normalized tracer uptake was converted to oxygen partial pressure (pO_2) and hypoxic target volumes (HTVs) were segmented using a threshold of 10 mmHg. Uniform doses required to overcome the hypoxic resistance in the target volumes were calculated based on a previously proposed method taking into account the effect of interfraction reoxygenation, for fractionation schedules ranging from extremely hypofractionated stereotactic body radiotherapy (SBRT) to conventionally fractionated radiotherapy.
Results: Gross target volumes ranged between 6.2 and 859.6 cm^3, and the hypoxic fraction $\leq$ 10 mmHg between 1.2% and 72.4%. The calculated doses for overcoming the resistance of cells in the HTVs were comparable to those currently prescribed in clinical practice as well as those previously tested in feasibility studies on dose escalation in NSCLC. Depending on the size of the HTV and the distribution of pO_2, HTV doses were calculated as 43.6–48.4 Gy for a three-fraction schedule, 51.7–57.6 Gy for five fractions, and 59.5–66.4 Gy for eight fractions. For patients in whom the HTV pO_2 distribution was more favorable, a lower dose was required despite a bigger volume. Tumor control probability was lower for single-fraction schedules, while higher levels of tumor control probability were found for schedules employing several fractions.
Conclusions: The method to account for heterogeneous and dynamic hypoxia in target volume segmentation and dose prescription based on ^{18}F-HX4-PET imaging appears feasible in NSCLC patients. The distribution of oxygen partial pressure within HTV could impact the required prescribed dose more than the size of the volume. [https://doi.org/10.1002/mp.13514]

Key words: dose painting, fractionation, hypoxia

1. INTRODUCTION

The field of radiotherapy is rapidly evolving with respect to physics, biology, and technology. While the technical development has allowed for the exploration of highly advanced treatments with increasing biological effectiveness,[1] research has also been focused on ways of increasing the efficiency of routine treatment techniques by targeting the tumor microenvironment.[2] As the therapeutic portfolio is continuously growing, the ability to consider and evaluate key radiobiological processes that are likely to govern the outcome of a treatment becomes increasingly important. Thus, in order to truly advance the practice of radiotherapy, crucial characteristics of the tumor microenvironment in conjunction with the treatment regimen need to be carefully studied.

One of the most important features of the tumor microenvironment with respect to radioresistance is hypoxia, since the isoeffective dose in hypoxic conditions could be up to three times higher than in normoxic conditions as quantified by the oxygen enhancement ratio.[3] Poor oxygenation has been well established to substantially increase the radioresistance of tumors and impact negatively on the outcome of radiotherapy.[4] In spite of this, there is currently no generally accepted approach for hypoxia mitigation in radiotherapy, and pretreatment imaging of hypoxia is part of the clinical routine only in very few centers around the world.[5] However, several advanced therapeutic approaches to overcome the issue of hypoxia have been investigated, including dose painting. One tumor type in which dose painting has been frequently investigated is nonsmall cell lung cancer (NSCLC). In general, lung cancer has poor prognosis and conventionally fractionated radiotherapy has been found to be inefficient in achieving local control in these patients.[6] In pursuit of an alternative treatment strategy with increased biological effectiveness, stereotactic body radiotherapy (SBRT) has been successfully applied to treat NSCLC with the majority of schedules ranging from one to ten fractions.[7–9] However, a high prevalence of hypoxia that varies dramatically in degrees between patients has been observed in NSCLC in particular.[10] Furthermore, studies investigating the evolution of hypoxia in these tumors over time have also shown that the tumor microenvironment is far from static in NSCLC patients,[11] and the importance of taking into account a heterogeneous and dynamic tumor oxygenation in SBRT of NSCLC has been previously demonstrated.[12]

In light of the dynamic nature of tumor oxygenation,[13] the challenges in radiotherapy of lung cancer driving the treatments to extreme hypofractionation warrant a robust method of evaluating the impact of fractionation on the outcome of these treatments with respect to tumor hypoxia, in particular. This is of high relevance for identifying SBRT fractionation schedules that could be preferred to others from the point of view of hypoxia and interfraction reoxygenation. It was the purpose of this study to investigate the impact of fractionation in hypoxia dose painting in NSCLC, based on the conversion of tracer uptake of a novel hypoxia positron emission tomography (PET) tracer, ^{18}F-HX4, to oxygen partial pressure.

2. MATERIALS AND METHODS

A previously developed function for converting normalized tracer uptake to oxygen partial pressure (pO_2) was applied to HX4-PET imaging data of 19 NSCLC patients. The expression for performing this conversion was originally derived based on experimental measurements of the normalized tracer uptake and the oxygen partial pressure pO_2.[14,15] This expression relates the normalized uptake, $Uptake_{norm,i}$, in each voxel i to the $pO_{2,i}$ in that voxel as:

$$Uptake_{norm,i} = A - \frac{B \cdot pO_{2,i}}{C + pO_{2,i}} \tag{1}$$

where A, B, and C are tracer-specific parameters that have been derived for ^{18}F-HX4 as $A = 10.9$, $B = 10.7$, and $C = 0.1$.[16] The first step is thus to normalize the uptake to obtain $Uptake_{norm,i}$. In each individual patient, a reference volume that contains normal, well-oxygenated tissue is delineated. The average value of the PET signal intensity in this volume is calculated and assumed to correspond to 60 mmHg, an oxygen partial pressure that could be expected in normoxic tissues[17]:

$$Uptake_{ref} = A - \frac{B \cdot 60}{C + 60} \tag{2}$$

All uptake values are normalized by $Uptake_{ref}$ and Eq. (1) is subsequently used to perform the conversion to pO_2. In the present paper, the aortic arch was considered as the reference volume in accordance with previous studies on hypoxia dose painting based on ^{18}F-HX4.[18,19] The resulting three-dimensional, heterogeneous distribution of pO_2 for each patient can be used for segmentation of target volumes as well as for quantifying the hypoxia-induced radioresistance of the tumor for dose painting purposes. In this way, hypoxic target volumes (HTV) were segmented in each of the 19 patients based on a pO_2 threshold of 10 mmHg. This value is in the upper limit of what is conventionally considered for the hypoxic threshold (i.e., 2.5–10 mmHg[20]) and could, therefore, be considered the safest approach with respect to ensuring the inclusion of the clinically relevant hypoxia in the hypoxic target volume. The segmented volumes were considered in relation to the clinical gross target volume (GTV).[16,19] If the HTV partly extended outside of the GTV, the GTV was adjusted to include the HTV in accordance with the expected course of action in a similar situation in the clinic. In some cases, this also inferred adjusting the clinical target volume (CTV) to encompass the new GTV. Subsequently, the HTV was considered a target for hypoxia-based dose painting, and the prescribed uniform dose required for 95% tumor control probability was calculated according to the method proposed by Toma-Dasu et al.[14] In this method, the conversion of normalized uptake to oxygen partial pressure is followed by the calculation of a voxelized map of dose-modifying factors (DMFs).[14,15,21] The probability of tumor clonogenic cell survival in each voxel is then calculated based on a radiobiological model of cell survival such as the linear-quadratic (LQ) model, in which the radiosensitivity parameters α and β are modified according to the DMFs. Conversely, a desired level of cell survival or, rather, tumor control probability can be assumed, and the dose $\hat{D}(\boldsymbol{r})$ required in each voxel at position $\boldsymbol{r}$ to achieve this probability (P) can be calculated as:

$$\hat{D}(\boldsymbol{r}) = n\frac{\alpha(\boldsymbol{r})}{2\beta(\boldsymbol{r})}\left[\sqrt{1+\frac{1}{n}\frac{4\beta(\boldsymbol{r})}{\alpha^2(\boldsymbol{r})}\ln\left(\frac{V_\rho}{-\ln P}\right)}-1\right] \tag{3}$$

where $\alpha(\boldsymbol{r})$ and $\beta(\boldsymbol{r})$ are the linear-quadratic radiosensitivity parameters, modified to depend on the pO_2, n is the number of fractions, and ρ is the density of clonogenic cells in the whole tumor volume V.[14,15] Depending on the distribution of pO_2 in the volume, Eq. (3) could result in a highly heterogeneous dose distribution that will be successful in controlling the tumor only if (a), the dose distribution is physically and technically feasible to deliver with high accuracy under the clinically accepted constraints for the normal tissue and the organs at risk, and (b), the tumor oxygenation remains exactly the same as represented in the original PET image. While the former is debatable, the tumor oxygenation is certainly expected to change between the time point of imaging and the treatment due to fluctuations in acute hypoxia.[13] This is equally well expected to occur between fractions throughout the treatment, warranting the inclusion of this effect in the calculation of the dose to be delivered. Under the conservative assumption that no global improvement is to be expected, the local changes in the tumor oxygenation will not affect the average pO_2 or, correspondingly, the average radiosensitivity. Thus, the random variations in acute hypoxia could be considered to correspond to a variance around the average radiosensitivity. Consequently, an average dose $\bar{D}$ with a variance σ_D^2 corresponding to the heterogenous dose distribution can be calculated. Based on a desired level of tumor control probability (P), a homogeneous prescribed dose D_{pres} can then be calculated as:

$$D_{pres} = \frac{\bar{D}}{\left[1 - \frac{\gamma}{2P(\bar{D})}\left(\frac{\sigma_D}{\bar{D}}\right)^2\right]} \tag{4}$$

where γ is the normalized slope of the dose–response curve corresponding to a homogeneous irradiation. While the resulting dose prescription is uniform, the heterogeneity in pO_2 on voxel level within the HTV is hence taken into account.[14,15] To ensure local control, the whole CTV has to be considered. The method for calculating the prescribed dose to the HTV was, therefore, applied also to the gross tumor volume (GTV) excluding the HTV, and the CTV excluding the GTV, respectively (Fig. 1). By segmenting the tumor in this way, the uniform dose prescription can be performed for individual subvolumes each with a more homogeneous radiosensitivity than in the whole tumor volume.

By varying the number of fractions, n, in Eq. (3), a range of fractionation schedules was considered in the present study. Given the increasing use of SBRT and failure of conventionally fractionated schedules in NSCLC, the analysis was focused on schedules employing between 1, 3, 5, 8, and 10 fractions. For comparison with the results of Even and colleagues,[18] n = 24 fractions were also considered, as well as a conventionally fractionated treatment of 30 fractions. For the purposes of the current study, calculations were performed for all fractionation schedules for each tumor regardless of the tumor volume and location.

Equation (4) was initially introduced under the assumption of several changes in radiosensitivity of the cells due to local interfractional fluctuations of acute hypoxia. Its validity could thus be questioned for hypofractionated treatments. The calculated prescribed doses were, therefore, evaluated with respect to the level of control they would ensure for different fractionation schedules by calculating the tumor control probability (TCP) in each target volume V divided into N voxels containing the same number of cells N_{vox} as:

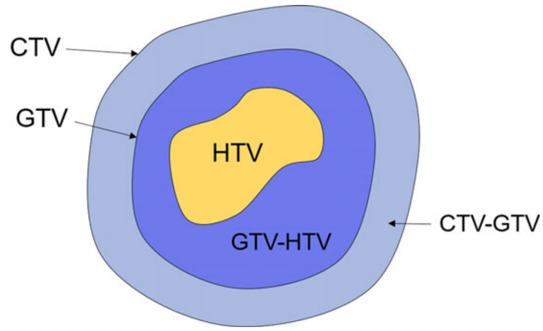

FIG. 1. Illustration of the target volumes considered for homogeneous dose prescription: clinical target volume (CTV), gross target volume (GTV), hypoxic target volume (HTV), the GTV not containing the HTV (GTV-HTV), and the CTV not containing the GTV (CTV-GTV). [Color figure can be viewed at wileyonlinelibrary.com]

$$TCP = \prod_{i=1}^{N} exp(-N_{vox}SF_i) \tag{5}$$

where SF_i is the surviving fraction in voxel i given by:

$$SF_i = \prod_{k=1}^{n} exp\left[-\frac{1}{n}\left(\frac{\alpha}{DMF_{i,k}}D_{pres} + \frac{\beta}{DMF_{i,k}^2}\frac{D_{pres}^2}{n}\right)\right] \tag{6}$$

with $DMF_{i,k}$ corresponding to the pO_2-dependent dose-modifying factor in voxel i and fraction k,[21] α and β to the linear-quadratic model parameters for the corresponding pO_2 conditions, and n to the number of fractions. To include the effects of interfraction reoxygenation in the calculation of TCP for the schedules employing more than one fraction, the $DMF_{i,k}$ in Eq. (6) were randomly resampled from the three-dimensional distribution mimicking the fluctuations in radiosensitivity related to changes in acute hypoxia. As a conservative approach with respect to achieving local control, no global improvement in the tumor oxygenation was assumed.

For all calculations, a uniform density of clonogenic cells of 10^9 cm^{-3} was assumed in all target volumes. The numerical values of the generic parameters used in Eqs. (3) and (4) were $\alpha = 0.35$ Gy^{-1}, $\alpha/\beta = 10$ Gy, $\gamma = 4$.[22,23]

3. RESULTS

For the patients included in this study, the GTVs ranged between 6.2 and 859.6 cm^3, with an average and median size of 150.8 and 101.7 cm^3, respectively. In Fig. 1, the target volumes considered for dose painting are illustrated, and in Fig. 2, examples of the segmented HTVs are shown for four of the patients. While a single HTV was observed in several of the patients as illustrated in Fig. 1, there were also cases in which several volumes with $pO_2 < 10$ mmHg were found. Regardless of the spatial distribution of voxels $\leq$ 10 mmHg, the total HTV volume in each patient was considered for the calculation of the prescribed doses. As previously mentioned, the GTV was adjusted to fully encompass the HTV contained

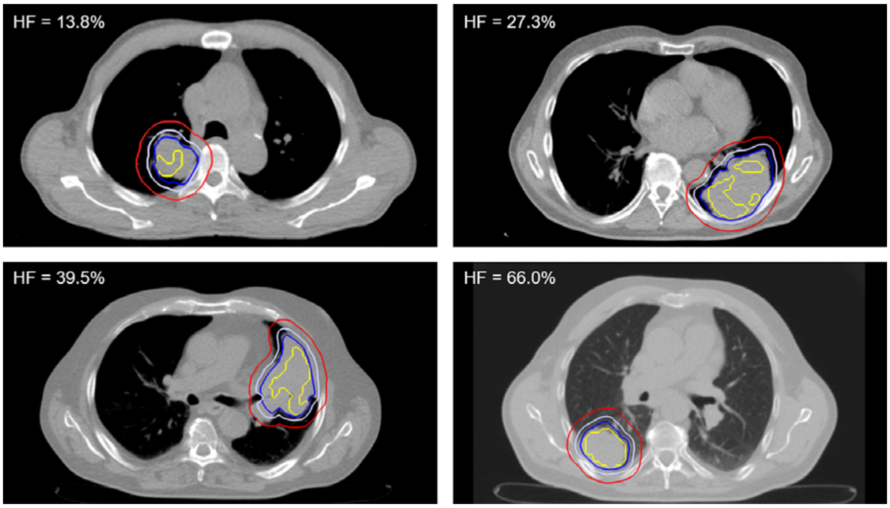

FIG. 2. Examples of segmented hypoxic target volumes (yellow) in the gross target volume (blue), as well as the clinical target volume (purple) and planning target volume (red) in four of the patients. The estimated hypoxic fraction (HF) in each case is indicated in the panels. [Color figure can be viewed at wileyonlinelibrary.com]

in the planning target volume (PTV). In a majority of the patients (11/19), the adjusted GTV was $\leq$1% larger than the original GTV, and in only 5 of 19 patients, the adjusted GTV was more than 1% but less than 5% larger than the originally delineated volume. The largest change of 74% was observed in patient 7. This patient had the smallest GTV in the entire cohort of only 6.2 cm^3, which was adjusted to 10.7 cm^3 to encompass the 7.8 cm^3 HTV.

Table I shows the uniform prescribed dose to the HTV, the GTV-HTV, and the CTV-GTV for the 19 patients included in the study for the range of fractionation schedules considered. Patient 1 was excluded due to the negligible hypoxic target volume of 0.1 cm^3. For all evaluated patients (patients 2–19) with HTVs of 0.8–84.5 cm^3, the HTV dose was consistently higher than both the GTV-HTV and the CTV-GTV doses. This could indicate that segmentation based on hypoxia PET imaging is warranted, especially for cases in which the size of the HTV and the pO_2 distribution result in a required prescribed dose that is substantially higher than what is needed in the remainder of the GTV and the CTV. In patient 14, for example, the HTV dose for a five-fraction treatment is more than 12 Gy higher than the dose to the CTV-GTV (56.9 and 44.3 Gy, respectively), comparable to one fraction in a typical five-fraction SBRT treatment.[9] The need for segmentation could be further demonstrated by considering the results for a more conventional approach in which the treatment consists of 30 fractions. For such a schedule, the total doses calculated correspond to a fractional dose of 2.8 Gy or higher in 13 of the 18 evaluated patients. While this is a dose that would most likely be feasible to deliver to a tumor subvolume such as an HTV,[24,25] it could be challenging to deliver as a uniform dose to the entire PTV within the limits of normal tissue toxicity constraints.

Interestingly, although the HTV is nearly identical in absolute size in patients 14 and 15, a higher dose is required in patient 14. This can be explained by considering the distribution of oxygen partial pressure within the HTVs, shown in Fig. 3 for patients 2–19 (in patient 1, the HTV is virtually zero). Indeed, in patient 14 the histogram displays a pO_2 distribution that is shifted toward lower values compared with patient 15, a difference that is reflected in the calculated dose. In fact, the prescribed dose for patient 14 is even higher than for patient 19, in which the largest HTV of 84.5 cm^3 was found, (to be compared with a volume of 61.1 cm^3 in patient 14). Thus, considering the distribution of oxygen partial pressure within the segmented HTV as opposed to just the size of the volume could lead to a difference in the subsequent dose prescriptions that might ultimately reflect on the treatment outcome.

Table II shows the TCP in the HTV for the prescribed doses in Table I. For all multifraction schedules, a TCP higher than the specified TCP of 95% is achieved. For the single-fraction schedule, a TCP of only 87.6% and 88.7% is obtained in patients 12 and 14, respectively. In these patients, the least favorable oxygen partial pressure distributions were found (Fig. 3), indicating the importance of considering not only the size of the HTV but also the distribution of pO_2. For three fractions, the TCP increases for all patients, with the largest increase seen in patients 12 and 14 from 87.6% to 98.2% in patient 12, and from 88.7% to 97.0% in patient 14. This could indicate that fractionated rather than single-fraction SBRT is preferable in tumors with unfavorable pO_2 distributions.

4. DISCUSSION

The potential for improving the outcome of radiotherapy by using functional imaging to identify and subsequently target tumor subvolumes believed to contain more radioresistant cells was first proposed almost two decades ago by Ling and colleagues.[26] Since then, various strategies to perform dose painting have been proposed ranging from dose painting by

TABLE I. The uniform prescribed dose for 95% tumor control probability to the hypoxic target volumes (HTV), gross target volume (GTV)-HTV, and the clinical target volume (CTV)-GTV for patients 2–19 assuming a treatment consisting of 1, 3, 5, 10, 24, or 30 fractions and a uniform clonogen density of 10^9 cm^{-3}. Patients are ordered according to the physical size of the HTV.

Patient	Target volume	Volume (cm^3; % of GTV)	D_{pres} (Gy)						
			1 fraction	3 fractions	5 fractions	8 fractions	10 fractions	24 fractions	30 fractions
2	HTV	0.8 (1.6)	28.7	44.0	52.3	60.3	64.1	77.7	80.7
	GTV-HTV	49.8	25.8	39.6	47.1	50.6	57.7	70.0	67.2
	CTV-GTV	55.9	24.3	37.1	44.0	54.3	53.7	64.8	72.7
3	HTV	1.4 (1.2)	29.3	45.1	53.7	61.9	65.8	80.1	83.2
	GTV-HTV	112.5	26.0	40.0	47.6	51.4	58.4	71.1	68.5
	CTV-GTV	151.6	24.6	37.6	44.7	55.0	54.6	66.0	73.8
4	HTV	2.9 (1.9)	29.2	44.8	53.4	61.6	65.5	79.6	82.7
	GTV-HTV	146.1	26.2	40.3	47.9	51.6	58.8	71.5	68.8
	CTV-GTV	89.9	24.7	37.8	44.9	55.3	54.8	66.3	74.3
5	HTV	4.4 (38.9)	29.2	44.7	53.1	61.1	64.8	78.4	81.3
	GTV-HTV	6.9	26.0	39.8	47.2	49.3	57.7	69.7	65.1
	CTV-GTV	17.5	23.8	36.3	43.0	54.3	52.3	62.9	72.3
6	HTV	5.8 (13.8)	29.0	44.4	52.8	60.8	64.6	78.4	81.4
	GTV-HTV	36.0	26.0	39.9	47.4	50.0	58.1	70.4	66.4
	CTV-GTV	43.8	24.0	36.7	43.5	54.7	53.1	64.0	73.1
7	HTV	7.8 (72.4)	28.5	43.5	51.7	59.5	63.2	76.3	79.1
	GTV-HTV	3.0	26.8	41.0	48.7	51.1	59.4	71.8	67.4
	CTV-GTV	11.9	24.7	37.6	44.5	56.0	54.1	65.0	74.5
8	HTV	11.1 (17.9)	29.8	45.8	54.5	62.8	66.7	81.0	84.1
	GTV-HTV	51.1	26.6	40.7	48.5	51.6	59.4	72.1	68.5
	CTV-GTV	66.6	24.7	37.8	44.8	55.9	54.7	66.1	74.8
9	HTV	11.2 (34.3)	29.5	45.2	53.8	61.9	65.8	79.7	82.7
	GTV-HTV	21.5	26.1	40.0	47.6	50.4	58.2	70.5	66.8
	CTV-GTV	34.2	24.2	37.0	43.9	54.8	53.5	64.4	73.2
10	HTV	12.1 (26.3)	29.3	44.9	53.4	61.5	65.4	79.3	82.3
	GTV-HTV	33.8	26.3	40.4	48.0	50.8	58.8	71.3	67.4
	CTV-GTV	56.8	24.4	37.2	44.2	55.3	53.9	65.0	74.1
11	HTV	36.8 (24.8)	30.1	46.1	55.0	63.4	67.4	82.0	85.2
	GTV-HTV	111.2	26.6	40.9	48.7	51.7	59.8	72.6	69.0
	CTV-GTV	101.1	24.7	37.8	45.0	56.2	55.0	66.5	75.5
12	HTV	44.8 (43.1)	31.5	48.4	57.6	66.4	70.6	85.8	89.1
	GTV-HTV	59.0	26.1	40.1	47.7	51.2	58.5	71.1	68.2
	CTV-GTV	78.4	24.5	37.5	44.5	55.1	54.4	65.7	73.8
13	HTV	47.3 (39.7)	30.4	46.7	55.6	64.1	68.2	82.8	86.0
	GTV-HTV	71.7	26.8	41.2	49.0	51.4	60.1	73.0	68.4
	CTV-GTV	80.8	24.6	37.6	44.6	56.5	54.5	65.9	75.8
14	HTV	61.1 (66.0)	31.2	47.8	56.9	65.6	69.8	84.7	87.9
	GTV-HTV	31.4	26.5	40.6	48.3	50.9	59.2	71.8	67.7
	CTV-GTV	47.2	24.4	37.3	44.3	55.7	54.0	65.2	74.6
15	HTV	62.2 (36.8)	30.2	46.5	55.3	63.8	67.9	82.6	85.8
	GTV-HTV	106.7	27.0	41.5	49.4	52.4	60.6	73.7	69.8
	CTV-GTV	105.2	25.0	38.3	45.5	57.0	55.6	67.3	76.5
16	HTV	63.2 (7.4)	31.0	47.8	57.0	65.9	70.1	85.6	89.0
	GTV-HTV	796.8	26.9	41.4	49.3	53.3	60.7	74.1	71.5
	CTV-GTV	259.8	25.3	38.8	46.2	57.0	56.7	68.8	77.0
17	HTV	63.4 (16.9)	30.5	47.0	56.0	64.7	68.8	83.9	87.2
	GTV-HTV	312.2	27.2	41.8	49.9	53.1	61.3	74.7	71.1
	CTV-GTV	281.5	25.3	38.8	46.1	57.6	56.5	68.5	77.6

Table I. Continued.

Patient	Target volume	Volume (cm^3; % of GTV)	D_{pres} (Gy)						
			1 fraction	3 fractions	5 fractions	8 fractions	10 fractions	24 fractions	30 fractions
18	HTV	80.6 (27.3)	30.2	46.3	55.2	63.8	67.8	82.6	85.8
	GTV-HTV	214.3	27.2	41.8	49.8	52.3	61.2	74.5	69.9
	CTV-GTV	132.6	25.0	38.2	45.4	57.5	55.6	67.4	77.4
19	HTV	84.5 (39.5)	30.6	47.0	55.9	64.6	68.7	83.6	86.9
	GTV-HTV	129.7	26.9	41.4	49.3	52.1	60.5	73.6	69.6
	CTV-GTV	142.9	24.9	38.1	45.3	56.9	55.4	67.1	76.5

numbers (DPBN), in which the dose distribution is allowed to be highly heterogeneous, to dose painting by contours (DPBC), in which larger volumes are prescribed a uniformly escalated dose.[27] DPBN could be questioned both from the point of view of the physical and technical limitations in delivering highly heterogeneous dose distributions, as well as the sensitivity of such a distribution to potential temporal changes in the microenvironment that cannot be resolved in a PET image. DPBC could thus provide a superior alternative with respect to both feasibility and robustness, and hence treatment outcome.[14,28] In NSCLC, several studies have investigated dose painting based on different tracers such as ^{18}F-labeled flurorodeoxyglucose (FDG), fluoromisonidazole (FMISO), and flortanidazole (HX4).[18,29] Furthermore, several modeling studies investigated the influence of heterogeneous tumor hypoxia on the treatment outcome.[21,30–33] However, given the qualitative information obtained from PET imaging, the determination of the prescribed dose still presents a challenge to the concept of dose painting in general. While the relationship between increased tumor metabolism, as reflected by FDG uptake, and radiosensitivity has not been elucidated, the relationship between oxygen partial pressure and relative radioresistance can be described mathematically. The method proposed by Toma-Dasu et al.[14,15], and used in this work, is based on this relationship.

By converting the normalized tracer uptake to pO_2, subvolumes can be delineated based on a hypoxic rather than an uptake threshold, and the dose that is required in order to overcome the resistance resulting from the pO_2 distribution within that volume can be calculated.[14,15] It has to be mentioned, however, that the mathematical expression in Eq. (4) used to calculate the homogeneous dose to be prescribed starting from a heterogeneous dose calculated at voxel level has a generic character and it depends on the standard deviation of these dose values. The heterogeneous dose distribution could be related to heterogeneous radiosensitivity of the cells in different voxels due to multiple reasons, one of them being the spatially heterogeneous oxygenation, but not exclusively. The expression for calculating the prescribed homogeneous dose, therefore, includes the standard deviation of the heterogeneous dose because of variations in radiosensitivity that could have many underlaying causes. Given the general character of the mathematical expression, one could say that the prescription dose is based on variations in radiosensitivity within a given interval. In this study, the definition of this interval was based on the hypothesis that the dominant factor leading to a variation in radiosensitivity is acute hypoxia. Thus, the prescribed homogeneous dose will ensure the targeted control probability as long as the spatial and temporal variations in radiosensitivity are within the given interval, regardless of the underlying causes. As can be seen in Eq. (4), the resulting uniform prescribed dose is always larger than the average dose required based on the pO_2 distribution. This can be explained by the fact that in a volume with heterogeneous sensitivity, the average dose required will correspond to underdosing the more resistant areas that cannot be compensated by overdosing the sensitive areas.[22] While this is also true for the prescribed dose (which will not correspond to the maximum dose required either), the random fluctuations in acute hypoxia expected to occur between fractions[13] will cause the "effective" radiosensitivity distribution — and consequently, the corresponding dose distribution — to become narrower. A narrow distribution of the radiosensitivity can also be expected in the better oxygenated remainder of the target volume (GTV-HTV, and CTV-GTV), in which the dose is calculated separately using the proposed method. In addition to the benefit in considering subvolumes with similar radiosensitivity as opposed to the whole tumor, the results of this work indicate the importance of considering the distribution of pO_2 *within* the HTV. This is demonstrated by a higher total dose required for a volume with a less favorable oxygen partial pressure distribution than in larger volumes with generally higher pO_2.

In light of the previous work on hypoxia dose painting by Even and colleagues,[18] the uniform prescribed doses calculated in this work could be considered clinically feasible with respect to the normal tissue toxicity constraints. Furthermore, the calculated doses corresponding to typical SBRT fractionation schedules (i.e., 1–10 fractions) are comparable to what is prescribed in the clinic. For example, in patients 12–19 with the largest HTVs of 44.8 to 84.5 cm^3, the prescribed doses were calculated as 46.3–48.4 Gy for three fractions, 55.2–57.6 Gy for five fractions, and 63.8–66.4 Gy for eight fractions. These results could be compared with the work of Baumann et al.[8] prescribing 45 Gy in three fractions to the 67% isodose and achieving local control rates exceeding 90%. Similarly, Haasbeek et al.[9] prescribed 60 Gy in eight fractions to the 80% isodose and observed a 3-yr local control

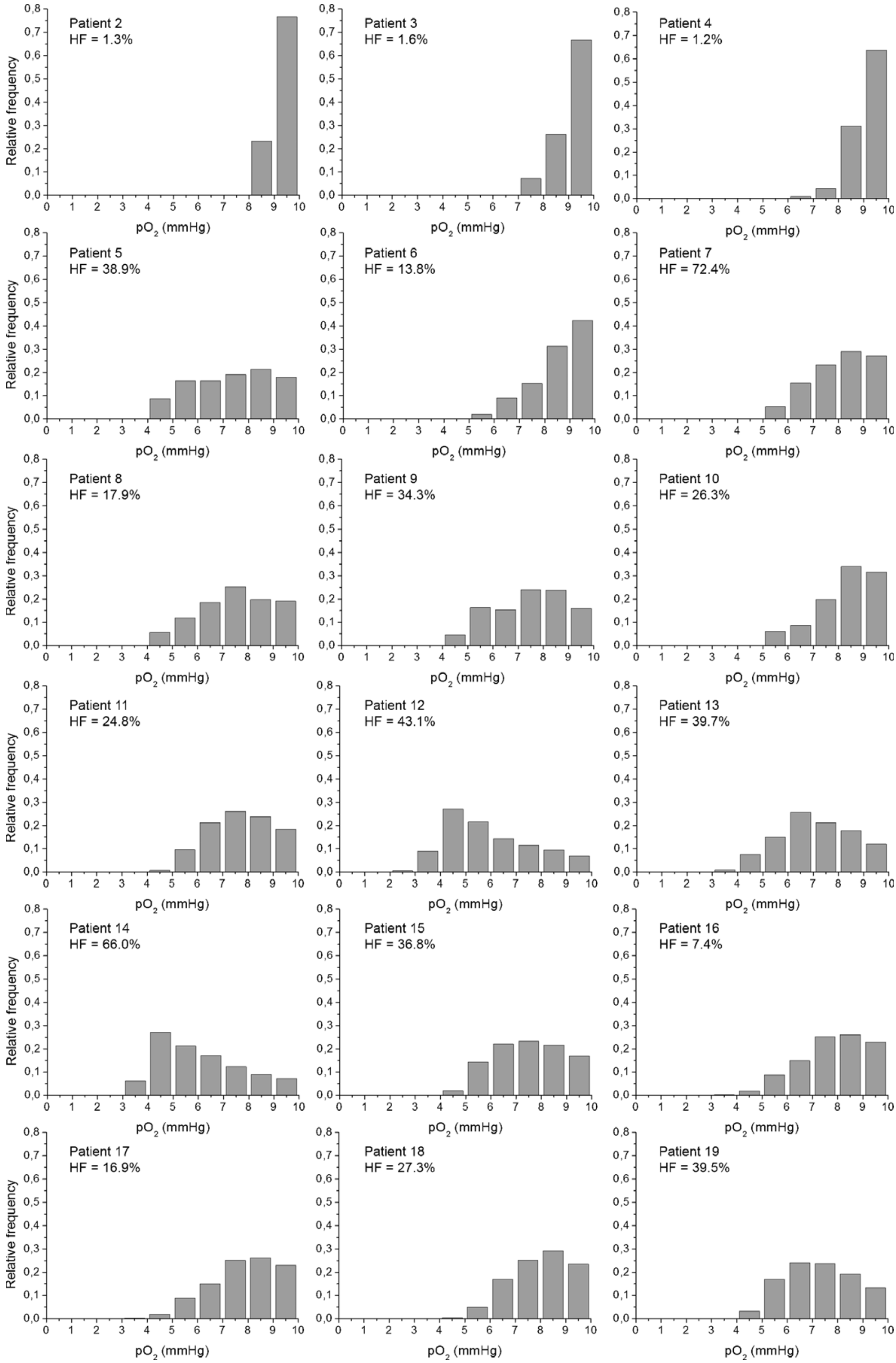

FIG. 3. Oxygen partial pressure histograms in the hypoxic target volume (HTV) for patients 2–19 (the histogram for patient 1 was excluded from this figure due to the negligible size of the HTV).

TABLE II. The uniform prescribed dose for 95% tumor control probability to the hypoxic target volumes (HTV) and the corresponding tumor control probability (TCP) calculated using Eqs. (3) and (4) for a uniform clonogen density of 10^9 cm^{-3}. Patients are ordered according to the physical size of the HTV.

	1 fraction		3 fractions		5 fractions		8 fractions	
Patient	D_{pres} (Gy)	TCP (%)	D_{pres} (Gy)	TCP (%)	D_{pres} (Gy)	TCP (%)	D_{pres} (Gy)	TCP (%)
2	28.7	100.0	44.0	100.0	52.3	100.0	60.3	100.0
3	29.3	100.0	45.1	100.0	53.7	100.0	61.9	100.0
4	29.2	100.0	44.8	100.0	53.4	100.0	61.6	100.0
5	29.2	97.2	44.7	99.2	53.1	99.3	61.1	99.4
6	29.0	99.5	44.4	99.7	52.8	99.7	60.8	99.7
7	28.5	97.5	43.5	98.5	51.7	98.6	59.5	98.6
8	29.8	98.2	45.8	99.5	54.5	99.6	62.8	99.6
9	29.51	97.4	45.2	99.1	53.8	99.3	61.9	99.3
10	29.3	99.0	44.9	99.5	53.4	99.5	61.5	99.5
11	30.1	98.4	46.1	99.2	55.0	99.3	63.4	99.4
12	31.5	87.6	48.4	98.2	57.6	98.8	66.4	99.0
13	30.4	94.0	46.7	98.5	55.6	98.8	64.1	99.0
14	31.2	88.7	47.8	97.0	56.9	97.9	65.6	98.2
15	30.3	97.0	46.5	98.8	55.3	98.9	63.8	99.0
16	31.0	96.5	47.8	99.6	57.0	99.7	65.9	99.8
17	30.5	97.6	47.0	99.5	56.0	99.6	64.7	99.6
18	30.2	97.9	46.3	99.0	55.2	99.1	63.8	99.2
19	30.6	96.7	47.0	98.7	55.9	98.9	64.6	99.0

of 89%. The agreement between the clinically prescribed SBRT doses resulting in high levels of local control and the prescribed doses for 95% tumor control probability calculated here could contribute to the explanation of the success of SBRT in NSCLC even in presumably rather hypoxic tumors. As the prescription isodoses clinically employed could vary substantially, different outcomes of the treatments depending on the resulting dose distribution in relation to the microenvironment of the tumor could be expected. For example, with the dose prescription of 7.5 Gy $\times$ 8 to the isocenter with a PTV-encompassing isodose of at least 90% reported by Shirata et al.[34], parts of the tumor could receive only 54 Gy in eight fractions, which is several Gy below the HTV doses calculated in the present work for a treatment consisting of eight fractions. As it is not safe to assume that hypoxic regions are located in the center of the tumor where the highest doses would be delivered in SBRT,[35] the need for comprehensive pretreatment assessment of the tumor oxygenation in SBRT is further highlighted.

The details of the tumor oxygenation and its evolution throughout the treatment could also greatly impact on the treatment outcome. In NSCLC, conventional fractionation has failed to achieve satisfying levels of local control[6] while impressive results have instead been obtained with SBRT, even resulting in surgery as primary treatment strategy in these patients being challenged.[36,37] The striking outcome achieved with SBRT has fostered the pursuit for an optimal radiotherapy treatment approach in NSCLC in particular, as has been recently reviewed by Ruggieri et al.[38] In this respect, efforts have been focused on both tumor control and normal tissue toxicity, and considering both the dose and the fractionation.[39–41] In a modeling study simulating the SBRT treatment of hypoxic NSCLC tumors, the impact of interfraction reoxygenation was shown to result in almost identical isoeffective total doses for a three- and a five-fraction schedule.[12] This is in line with the work by Park and colleagues, showing a similar overall survival in 5600 NSCLC patients treated with either a three-, four-, or five-fraction SBRT.[42] While Ma and colleagues found no difference in clinical outcome in NSCLC patients treated with either a single- or three-fraction SBRT,[43] Huang et al.[44] concluded that a single fraction of 30 Gy was superior to 12 Gy $\times$ 4. However, in the modeling study by Huang and coworkers, the impact of tumor reoxygenation was not included as in the study by Lindblom et al. In addition, Huang et al. only included clinical data on NSCLC tumors of very limited size (<3 cm) in order to exclude the impact of tumor size. Their conclusions could thus be limited to small, well-oxygenated tumors. In addition to the expected benefit in local control from interfraction reoxygenation in fractionated as opposed to single-fraction SBRT, Jain et al.[40] compared the acute toxicity and quality of life in NSCLC patients treated with SBRT in either 4 or 11 days and found that patients treated for the longer period of 11 days fared better. In general, the collected work on the impact of treatment time, dose and fractionation in SBRT of NSCLC indicate that finding the optimal radiotherapy treatment strategy requires a multifaceted approach in which the most crucial aspects impacting on the overall outcome have to be taken into account. In the present study, the tumor control probability evaluated as described by Eqs. (5) and (6) indicate that fractionated rather than single-fraction SBRT treatments should be considered in order to maximize the

TCP, as also shown for neurosurgery treatments.[45] This was particularly pronounced in the two patients (12 and 14) in which the least favorable distributions of oxygen partial pressure were found. Based on the large interpatient variability in hypoxia observed in NSCLC[10] combined with intratumor heterogeneity in oxygenation in both time and space,[11,13] it is likely that individual patients would benefit from pretreatment assessment of their particular tumor oxygenation status. However, this is of course only valid under the assumption that there are clinically validated methods for adapting the treatment according to this information, and that the resulting treatment can be safely delivered with respect to the normal tissue toxicity and the potential motion of the tumor. The methodology employed in the current study could represent a promising strategy for quantitative dose prescription based on hypoxia PET imaging.

It has to be mentioned that the conversion of PET tracer uptake to pO_2 could be associated with several uncertainties. In addition to potential uncertainties related to the conversion itself, the use of PET imaging for any quantitative analysis requires correction for scatter and attenuation of the annihilation photons as well as for partial volume effects.[46] For imaging of the thoracic region, correction for respiratory motion may also be necessary.[47] It should, however, be pointed out that the uncertainties discussed here pertains to all use of PET imaging, and are not specific to the method employed in this study. Rather, the conversion to pO_2 should be considered only after all necessary corrections of the raw PET data have been performed. In patient 7, this might not have been the case as a relatively large HTV was observed resulting in an increase in the GTV from 6.2 to 10.7 cm^3 in order to encompass the 7.8 cm^3 HTV. Given the many steps from PET imaging to prescribed dose (conversion, segmentation, dose calculation) the accuracy of the conversion and subsequent dose calculation should be evaluated with respect to its application rather than by evaluating isolated steps of the chain. The critical question is, therefore, whether the doses calculated based on the model are enough to achieve local control, which should be assessed by comparing the predictions of the model with the outcome of patients treated according to clinical praxis. While the work presented in this paper demonstrates the potential in quantitative hypoxia dose painting based on radiobiological modeling, validation against clinical results prior to translating the results and methodology to the clinic is needed.

5. CONCLUSIONS

In this work, a radiobiological method for calculating the prescribed dose in tumor subvolumes segmented based on functional imaging of hypoxia was employed to investigate the impact of fractionation on the prescribed doses calculated, taking into account the dynamic nature of the tumor oxygenation. The importance of considering the pO_2 distribution in addition to the volume for dose prescription was demonstrated, indicating that hypoxia dose painting based on segmentation alone may not be sufficient with respect to achieving local control. The method resulted in prescribed doses that were similar to the clinical practice in SBRT of NSCLC for a range of fractions. Furthermore, the independent calculation of tumor control probability indicated that single-fraction SBRT could result in local control rates inferior to those achievable with fractionated SBRT. Clinical validation of this (as of any radiobiological modeling approach) is, however, required before the results of this work can be translated to the clinic.

ACKNOWLEDGMENTS

This work was partly funded by EU 7th framework ARTFORCE project. Financial support from the Cancer Research Funds of Radiumhemmet is also gratefully acknowledged.

CONFLICTS OF INTERESTS

None to declare.

[a)]Author to whom correspondence should be addressed. Electronic mail: emely.lindblom@fysik.su.se.

REFERENCES

1. Sokol O, Scifoni E, Tinganelli W, et al. Oxygen beams for therapy: advanced biological treatment planning and experimental verification. *Phys Med Biol*. 2017;62:7798–7813.
2. Jain S, Coulter JA, Butterworth KT, et al. Gold nanoparticle cellular uptake, toxicity and radiosensitisation in hypoxic conditions. *Radiother Oncol*. 2014;110:342–347.
3. Hall AJ, Giaccia EJ. *Radiobiology for the Radiologist*, 7th Ed., Vol. 166. Philadelphia, PA: Wolters Kluwer Health; 2011.
4. Brustugun OT. Hypoxia as a cause of treatment failure in non-small cell carcinoma of the lung. *Semin Radiat Oncol*. 2015;25:87–92.
5. Overgaard J. Hypoxic radiosensitization: adored and ignored. *J Clin Oncol*. 2007;25:4066–4074.
6. Onishi H, Araki T, Shirato H, et al. Stereotactic hypofractionated high-dose irradiation for stage I nonsmall cell lung carcinoma: clinical outcomes in 245 subjects in a Japanese multiinstitutional study. *Cancer*. 2004;101:1623–1631.
7. Hof H, Muenter M, Oetzel D, Hoess A, Debus J, Herfarth K. Stereotactic single-dose radiotherapy (radiosurgery) of early stage nonsmall-cell lung cancer (NSCLC). *Cancer*. 2007;110:148–155.
8. Baumann P, Nyman J, Hoyer M, et al. Outcome in a prospective phase II trial of medically inoperable stage I non-small-cell lung cancer patients treated with stereotactic body radiotherapy. *J Clin Oncol*. 2009;27:3290–3296.
9. Haasbeek CJA, Lagerwaard FJ, Antonisse ME, Slotman BJ, Senan S. Stage I nonsmall cell lung cancer in patients aged > or = 75 years: outcomes after stereotactic radiotherapy. *Cancer*. 2010;116:406–414.
10. Rasey JS, Koh WJ, Evans ML, et al. Quantifying regional hypoxia in human tumors with positron emission tomography of [18F]fluoromisonidazole: a pretherapy study of 37 patients. *Int J Radiat Oncol Biol Phys*. 1996;36:417–428.
11. Koh WJ, Bergman KS, Rasey JS, et al. Evaluation of oxygenation status during fractionated radiotherapy in human nonsmall cell lung cancers using [F-18]fluoromisonidazole positron emission tomography. *Int J Radiat Oncol Biol Phys*. 1995;33:391–398.
12. Lindblom E, Antonovic L, Dasu A, Lax I, Wersäll P, Toma-Dasu I. Treatment fractionation for stereotactic radiotherapy of lung tumours: a modelling study of the influence of chronic and acute hypoxia on tumour control probability. *Radiat Oncol*. 2014;9:149.

13. Ljungkvist ASE, Bussink J, Kaanders JH, Wiedenmann NE, Vlasman R, van der Kogel AJ. Dynamics of hypoxia, proliferation and apoptosis after irradiation in a murine tumor model. *Radiat Res*. 2006;165:326–336.
14. Toma-Daşu I, Daşu A, Brahme A. Dose prescription and optimisation based on tumour hypoxia. *Acta Oncol (Madr)*. 2009;48:1181–1192.
15. Toma-Dasu I, Uhrdin J, Antonovic L, et al. Dose prescription and treatment planning based on FMISO-PET hypoxia. *Acta Oncol (Madr)*. 2012;51:222–230.
16. Ureba A, Lindblom E, Dasu A, et al. Non-linear conversion of HX4 uptake for automatic segmentation of hypoxic volumes and dose prescription. *Acta Oncol*. 2017;57:485–490.
17. McKeown SR. Defining normoxia, physoxia and hypoxia in tumours-implications for treatment response. *Br J Radiol*. 2014;87:20130676.
18. Even AJG, Van Der Stoep J, Zegers CML, et al. PET-based dose painting in non-small cell lung cancer: comparing uniform dose escalation with boosting hypoxic and metabolically active sub-volumes. *Radiother Oncol*. 2015;116:281–286.
19. Lindblom E, Dasu A, Uhrdin J, et al. Defining the hypoxic target volume based on positron emission tomography for image guided radiotherapy - the influence of the choice of the reference region and conversion function. *Acta Oncol*. 2017;56:819–825.
20. Höckel M, Vaupel P. Tumor hypoxia: definitions and current clinical, biologic, and molecular aspects. *J Natl Cancer Inst*. 2001;93:266–276.
21. Toma-Dasu I, Dasu A. Modelling tumour oxygenation, reoxygenation and implications on treatment outcome. *Comput Math Methods Med*. 2013;2013:141087.
22. Brahme A. Dosimetric precision requirements in radiation therapy. *Acta Oncol (Madr)*. 1984;23:379–391.
23. Partridge M, Ramos M, Sardaro A, Brada M. Dose escalation for non-small cell lung cancer: analysis and modelling of published literature. *Radiother Oncol*. 2011;99:6–11.
24. Jeter M, Gomez D, Nguyen Q, et al. Simultaneous integrated boost for radiation dose escalation to the gross tumor volume with intensity modulated (photon) radiation therapy or intensity modulated proton therapy and concurrent chemotherapy for stage II to III non-small cell lung cancer: a Phase 1 Study. *Int J Radiat Oncol Biol Phys*. 2017;100:730–737.
25. Yang W, Zeng B, Qiu Y, et al. A dosimetric comparison of dose escalation with simultaneous integrated boost for locally advanced non-small-cell lung cancer. *Biomed Res Int*. 2017;2017:9736362.
26. Ling CC, Humm J, Larson S, et al. Towards multidimensional radiotherapy (MD-CRT): biological imaging and biological conformality. *Int J Radiat Oncol Biol Phys*. 2000;47:551–560.
27. Bentzen SM, Gregoire V. Molecular imaging-based dose painting: a novel paradigm for radiation therapy prescription. *Semin Radiat Oncol*. 2011;21:101–110.
28. Thorwarth D, Alber M. Implementation of hypoxia imaging into treatment planning and delivery. *Radiother Oncol*. 2010;97:172–175.
29. Vera P, Thureau S, Chaumet-Riffaud P, et al. Phase II study of a radiotherapy total dose increase in hypoxic lesions identified by 18F-misonidazole PET/CT in patients with non-small cell lung carcinoma (RTEP5 Study). *J Nucl Med*. 2017;58:1045–1053.
30. Petit SF, Dekker ALAJ, Seigneuric R, et al. Intra-voxel heterogeneity influences the dose prescription for dose-painting with radiotherapy: a modelling study. *Phys Med Biol*. 2009;54:2179–2196.
31. Mönnich D, Troost EGC, Kaanders JHAM, Oyen WJG, Alber M, Thorwarth D. Modelling and simulation of [18F]fluoromisonidazole dynamics based on histology-derived microvessel maps. *Phys Med Biol*. 2011;56:2045–2057.
32. Powathil G, Kohandel M, Milosevic M, Sivaloganathan S. Modeling the spatial distribution of chronic tumor hypoxia: implications for experimental and clinical studies. *Comput Math Methods Med*. 2012;2012: 410602.
33. Daşu A, Toma-Daşu I. Treatment modelling: the influence of micro-environmental conditions. *Acta Oncol (Madr)*. 2008;47:896–905.
34. Shirata Y, Jingu K, Koto M, et al. Prognostic factors for local control of stage I non-small cell lung cancer in stereotactic radiotherapy: a retrospective analysis. *Radiat Oncol*. 2012;7:182.
35. Bittner MI, Grosu AL. Hypoxia in head and neck tumors: characteristics and development during therapy. *Front Oncol*. 2013;3:223.
36. White A, Swanson SJ. Surgery versus stereotactic ablative radiotherapy (SABR) for early-stage non-small cell lung cancer: less is not more. *J Thorac Dis*. 2016;8:S399–S405.
37. Moghanaki D, Chang JY. Is surgery still the optimal treatment for stage I non-small cell lung cancer? *Transl Lung Cancer Res*. 2016;5: 183–189.
38. Ruggieri R, Stavrev P, Naccarato S, Stavreva N, Alongi F, Nahum AE. Optimal dose and fraction number in SBRT of lung tumours: a radiobiological analysis. *Phys Med*. 2016;44:188–195.
39. Lindblom E, Dasu A, Toma-Dasu I. Optimal fractionation in radiotherapy for non-small cell lung cancer - a modelling approach. *Acta Oncol (Madr)*. 2015;54:1592–1598.
40. Jain S, Poon I, Soliman H, et al. Lung stereotactic body radiation therapy (SBRT) delivered over 4 or 11 days: a comparison of acute toxicity and quality of life. *Radiother Oncol*. 2013;108:320–325.
41. Liu X-J, Lin X-T, Yin Y, Chen J-H, Xing L-G, Yu J-M. Determining the optimal dose prescription for the planning target volume with stereotactic body radiotherapy for non- small cell lung cancer patients. *Asian Pacific J Cancer Prev*. 2016;17:2573–2577.
42. Park H, Corso C, Rutter C, et al. Survival comparison of 3 versus 4-5 fractions for stereotactic body radiation therapy in stage i non-small cell lung cancer. *Int J Radiat Oncol Biol Phys*. 2015;93:S100.
43. Ma S, Serra L, Syed Y, Hermann G, Gomez-Suescun J, Singh AK. Comparison of single- and three-fraction schedules of stereotactic body radiation therapy for peripheral early-stage non-small-cell lung cancer. *Clin Lung Cancer*. 2017;19:e235–e240.
44. Huang B-T, Lu J-Y, Lin P-X, Chen J-Z, Li D-R, Chen C-Z. Radiobiological modeling analysis of the optimal fraction scheme in patients with peripheral non-small cell lung cancer undergoing stereotactic body radiotherapy. *Sci Rep*. 2015;5:18010.
45. Toma-Dasu I, Sandström H, Barsoum P, Dasu A. To fractionate or not to fractionate? That is the question for the radiosurgery of hypoxic tumors. *J Neurosurg*. 2014;121:110–115.
46. Adams MC, Turkington TG, Wilson JM, Wong TZ. A systematic review of the factors affecting accuracy of SUV measurements of SUV. *AJR Am J Roentgenol*. 2010;195:310–320.
47. Nehmeh SA, Erdi YE. Respiratory motion in positron emission tomography/computed tomography: a review. *Semin Nucl Med*. 2008;38: 167–176.